Journal of Fluorescence, Vol. 8, No. 1, 1998

Ground-State Complex Formation of Perylene with Pyromellitic Dianhydride Studied by Static Fluorescence Quenching

Horst Gebert,[1] Wolfgang Kretzschmar,[1] and Wolfgang Regenstein[1]

Received October 27, 1997; accepted January 5, 1998

The association of complex formation with static quenching in CT systems was investigated. Evaluation of the data made evident that the inner filter effect must be allowed for. Time-resolved and temperature-dependent stationary measurements of fluorescence led to the separation of dynamic and static quenching components. The static quenching constant is discussed with respect to the equilibrium constant of complex formation determined by absorption spectroscopy.

KEY WORDS: Charge transfer interaction; complex formation; fluorescence quenching; inner filter effect.

INTRODUCTION

Mulliken explained charge transfer (CT) complex formation by the superposition of an ionic bond structure and a covalent no-bond structure [1]. Absorption of the CT energy takes the complex to an excited state. Complex formation from molecular sites is controlled by the law of mass action.

The equilibrium constant and association enthalpy of the ionic bond structure can be derived from the concentration and temperature dependence of the CT absorption. Assuming a 1:1 complex formation, the molar equilibrium constant was calculated using the equation [2]

$$\frac{1}{K_{CT}} = \frac{\varepsilon_{DA} \cdot c_D \cdot c_A}{E} - c_D - c_A + \frac{E}{1\varepsilon_{DA}} \qquad (1)$$

where E is the absorbance, ε_{DA} is the decadic molar extinction coefficient of the complex, and 1 is the thickness of the cuvette, by variation of donor and acceptor concentrations c_D and c_A.

Considering the temperature dependence of the equilibrium constant K in the Gibbs–Helmholtz equation,

$$\Delta G = \Delta H - TS \qquad (2)$$

with

$$\Delta G = -RT \ln K \qquad (3)$$

it becomes possible to fix the thermodynamic quantities Gibbs reaction energy ΔG, reaction entropy S, and reaction enthalpy ΔH.

In order to account for fluorescence quenching by CT interaction, and analogously to the theory of Rehm and Weller [3], we propose the following scheme of reactions:

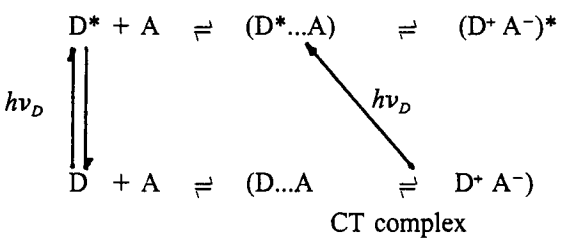

[1] Universität Potsdam, Institut für Physik, Am Neuen Palais 10, D-14469 Potsdam, Germany.

1053-0509/98/0300-0067$15.00/0

Consistently, the quenching of donor fluorescence is associated with the excitation of CT complexes.

The total quenching, i.e., the simultaneous occurrence of dynamic and static quenching, is approximately described by [4]

$$\frac{F^0}{F} \approx (1 + K_{dyn}\, c_Q)\,(1 + K_{stat}\, c_Q) \qquad (4)$$

The static quenching term applied here was derived as the first mathematical approximation from Perrin's statistical concept.

If we extend the concept and take a ground-state interaction into account, the static quenching constant will not be equal to the molar interaction volume v any more, as introduced by Perrin, but constitutes a product of v and an Arrhenius term including the Gibbs association energy ΔG_{stat},

$$K_{stat} = v \cdot \exp\left(-\frac{\Delta G_{stat}}{RT}\right) \qquad (5)$$

Time-resolved measurements allow separation of the dynamic portion of quenching from the total quenching. Application of the Stern–Volmer equation

$$\frac{\tau^0}{\tau} = 1 + K_{dyn} \cdot c_Q \qquad (6)$$

on the data determines the dynamic quenching constant K_{dyn}.

EXPERIMENTAL

Sample Preparation. Substances of investigations were perylene (Pe) as fluorophore and pyromellitic dianhydride (PMDA) as quencher dissolved in an ethanol/methanol mixture (4:1). The solvent permitted temperature-dependent measurements.

The solutions were not degassed since it was not our aim to determine experimentally absolute quantum yields but relative radiation intensities. Oxygen quenching, which accounts for a decrease in fluorescence of about 30%, was not given any further consideration because it affected each sample at a given temperature in the same way. As time-resolved measurements confirmed, the lifetime of the Pe fluorescence was lowered from 6.0 to 4.4 ns at room temperature, which is accounted for by the presence of dissolved molecular oxygen. These values are also found in the literature [5,6].

The Pe concentration was kept constant at a value of 10^{-5} mol L^{-1} for all fluorescence experiments, while the quencher concentration varied from 0 to 0.1 mol/L, ensuring that static quenching could be recognized and separated from fake quenching such as filter effects.

The concentrations of Pe were increased up to the limit of solubility for absorption experiments, since determination of the thermodynamic equilibrium constant of CT complex formation required variation of the electron-donor (Pe) concentration against a comparatively low concentration of electron-acceptor (PMDA), and vice versa.

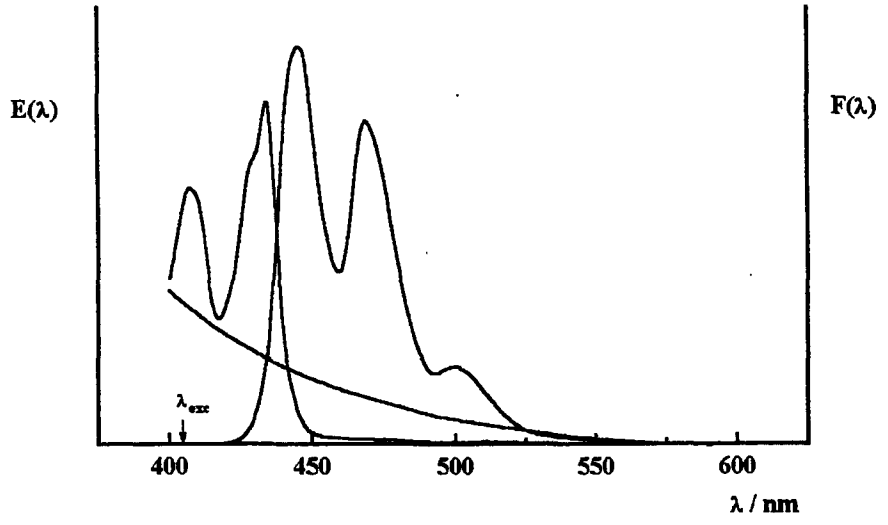

Fig. 1. Region of overlap of fluorescence and absorption spectra.

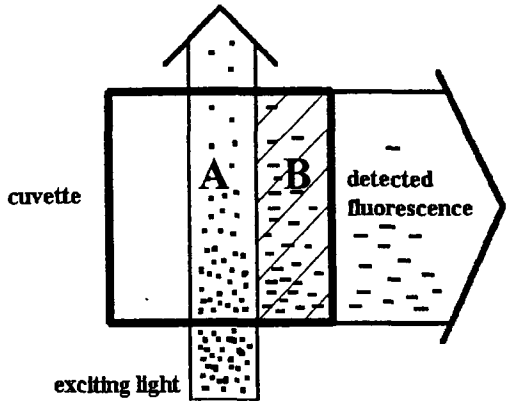

Fig. 2. (A) Illuminated region and intensity loss of exciting light in the cuvette. (B) Absorbing region (filter) and intensity loss of fluorescence.

Absorption. Spectra were recorded by a Lambda 19 (Perkin Elmer) spectrometer. A cryostat (SPECAC) was used for cooling in the temperature range from 120 to 300 K. The thickness of the cuvette was 3 cm.

Fluorescence. Steady-state fluorescence spectra were recorded with a commercial fluorescence spectrometer (Alphascan, Photon Technology International). Samples were excited at $\lambda_{exc} = 410$ nm (see Fig. 1) using a 75-W Xe lamp and single monochromators for wavelength separation of both the excitation light (bandwith, 4 nm) and the fluorescence light (spectral resolution, 3 nm). The samples were cooled in an Oxford cryostat (DN 1704). The temperature was measured and controlled by an autotuning temperature controller (Oxford ITC4) with an accuracy of 2 K. The luminescence was detected by a photomultiplier (TP1527; Hamamatsu) and measured with the photon-counting technique. Fluorescence decay curves were measured using the time-correlated single-photon counting technique and front-face illumination. The short focal length of the collecting lens ensures that only the fluorescence light emitted near the surface is detected, excluding influences of reabsorption and reemission. The excitation light source was a frequency-doubled dye laser (701; Coherent) synchronously pumped by a frequency-doubled, mode-locked Nd:YAG laser (2 W, 76 MHz; Antares 76 ML; Coherent). The repetition rate was reduced to 3.8 MHz by a 7200 cavity dumper. The samples were excited by pulses of about 5 ps and 355 nm using pyridine 2 as the laser dye. The fluorescence light was dispersed by a subtractive double monochromator (AMKO) and detected by a MCP-PMT R3809U (Hamamatsu). The overall instrumental response width using timing electronics from Tennelec and Ortec including a 8 K multichannel analyzer is 40 ps. The lifetimes were calculated by the software "Physfit" (Picoquant).

Correction for Inner Filter Effect (IFE). If the quencher exhibits absorbance at the wavelength of fluorophore excitation and/or over the fluorescence region, the data must be corrected for the IFE [7,8].

The IFE comprises two processes in succession with different consequences. The prefilter effect (PrFE) diminishes the incident light disposable for fluorescence excitation. Adding a second substance may cause an increase in absorbance, which in turn gives rise to the following. First, there is an additional intensity loss of excitation radiation along the light path through the cuvette. Second, from the total amount of light absorbed by any volume element, there is only a fraction available for fluorophore excitation (see Fig. 1), and it is only from this remaining fraction that, according to the actual quantum yield, emission can emerge.

For every quencher concentration the intensity of the emerging fluorescence has to be related to the light intensity which was actually absorbed by the fluorophore.

$$F = F_{det} \cdot \frac{E_F + E_Q}{E_F\,(1 - 10^{-E_t - E_0})} \qquad (7)$$

Equation (7) presumes that the total fluorescent volume is detected with equal efficiency (see Fig. 2).

Fluorescence succeeds the PrFE. Before detection the emitted light traverses a volume of wavelength-dependent absorption (see Fig. 2). In contrast to the PrFE, the PFE attenuates the intensity and, at the same time, distorts the fluorescence spectra. Quenching affects the fluorescence intensity alone. Consequently, quenched spectra are proportional to the unquenched spectrum. Since the average thickness of the absorbing volume changes with the actual concentration and geometric configurations inside the cuvette, it becomes impossible to fix one value of thickness that is generally valid. Instead, the average thickness is regarded as a varying geometric parameter in the mathematical analysis of spectra. Hence, the proportionality of fluorescence spectra remains the one and only criterion. The factor F_{post}/F_0 represents the PFE-corrected inverse quenching ratio.

$$F_{det}(\lambda, c_Q) = \frac{F_{post}}{F^0} \cdot F^0_{det}(\lambda) \cdot (1 - 10^{-\varepsilon_Q c_Q d}) \qquad (8)$$

In general, both corrections are applied. With quenching experiments, correction for the PFE comes first and delivers proportionality between the spectra. The quench-

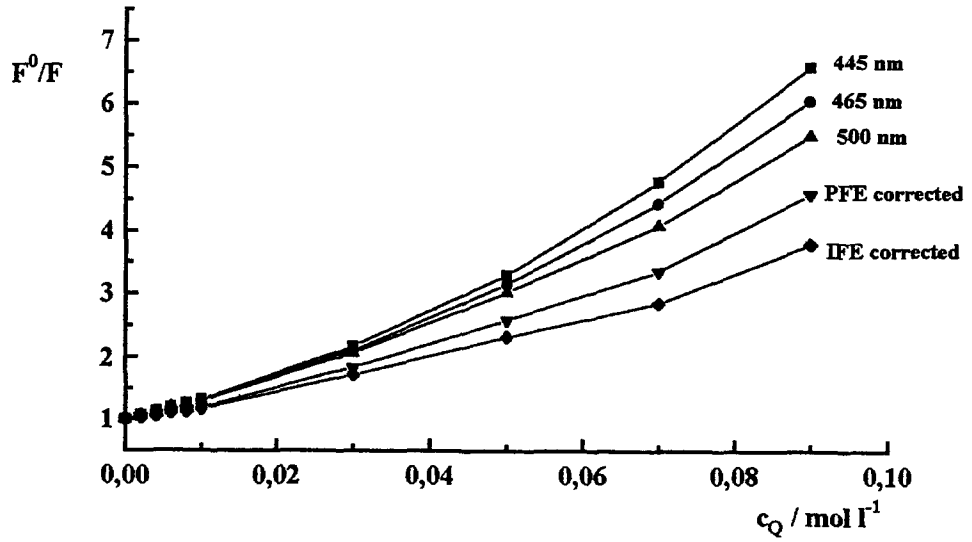

Fig. 3. Quenching plots for different observation wavelength, PFE-corrected, and IFE-corrected graphs.

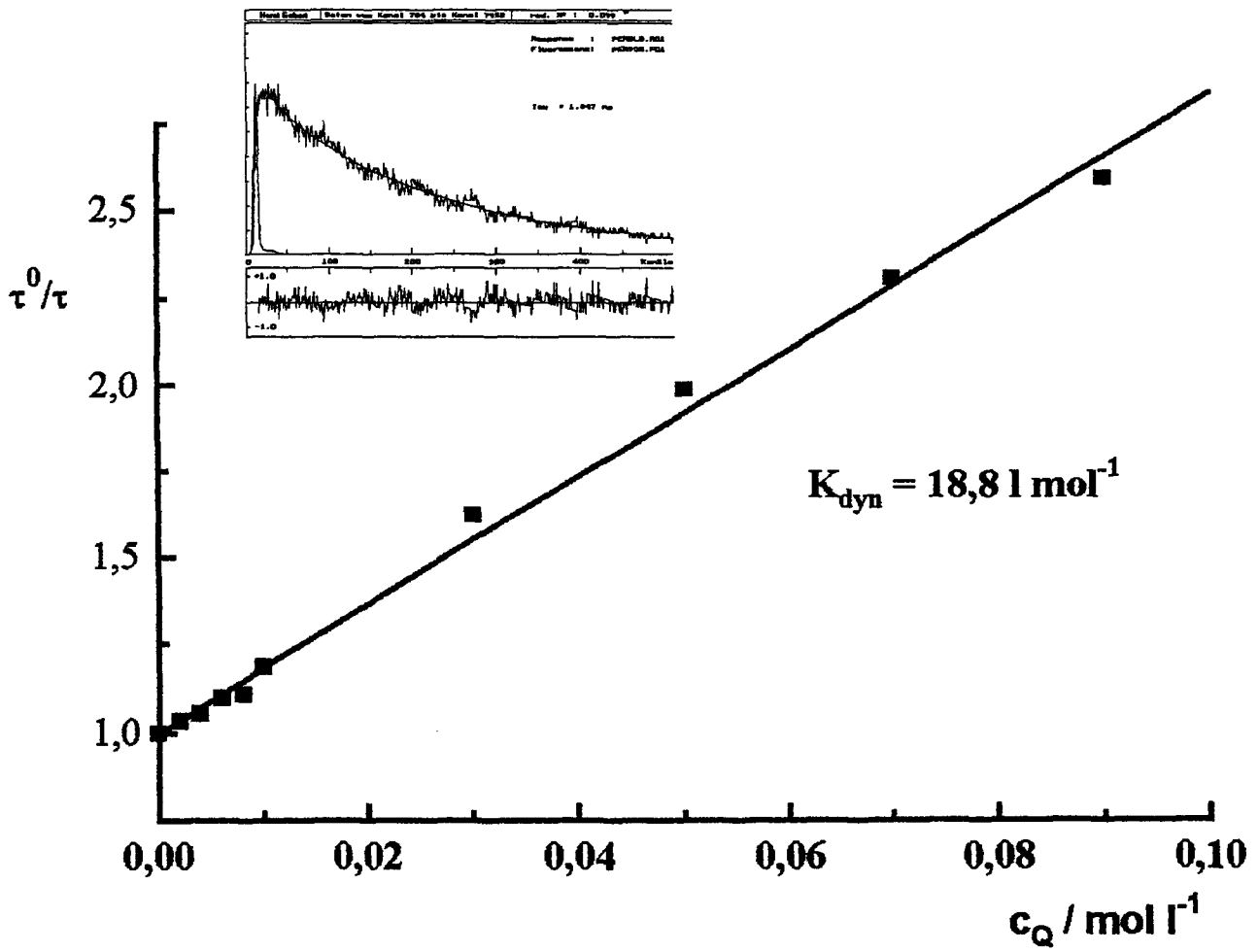

Fig. 4. Stern–Volmer plot of fluorescence lifetimes. Inset: Measured decay curve with system response and monoexponentially fitted curve.

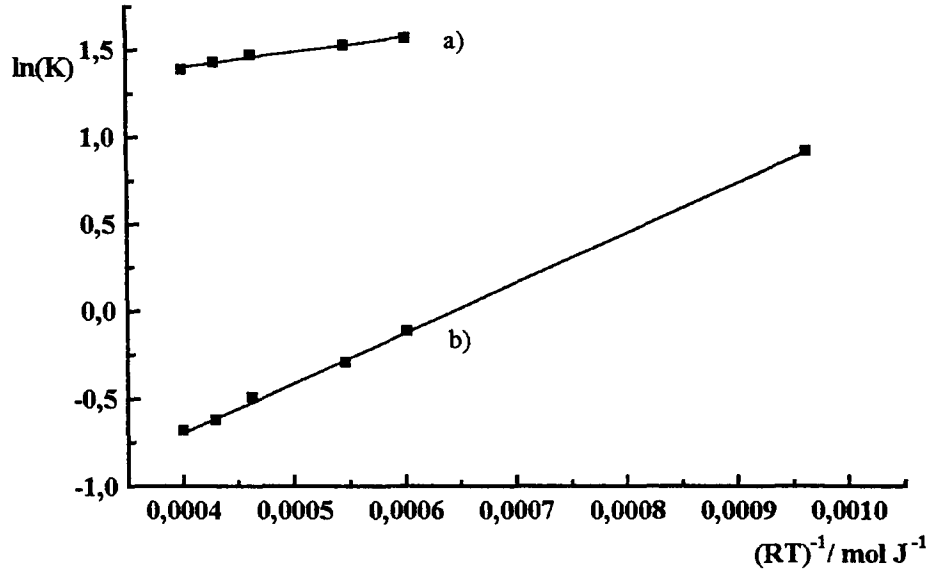

Fig. 5. Temperature dependence of the static quenching constant (a) and the constant of complex formation determined by absorption spectroscopy (b).

Table I.

	L mol^{-1}		
T (K)	K_{dyn}	K_{stat}	K_{CT}
300	18.8	4.0	0.50
280	12.3	4.2	0.55
260	7.8	4.4	0.60
220	2.4	4.6	0.75
200	1.0	4.8	0.90
125			2.50

ing ratio so obtained is then corrected for the PrFE according to the equation

$$\frac{F^0}{F} = \frac{F^0}{F_{post}} \cdot \frac{E_F\,(1 - 10^{-E_F})}{(E_F + E_Q)(1 - 10^{-E_F - E_Q})} \qquad (9)$$

RESULTS AND DISCUSSION

Figure 3 demonstrates the dependence of Stern–Volmer plots on the wavelength of observation. Over the region of Pe fluorescence the extinction coefficient of PMDA decreases monotonously with increasing wavelength (see Fig. 1). The absorption of fluorescence light by the quencher is subject to the same dependency. The influence of the PFE on the measured fluorescence becomes smaller toward longer wavelengths of observation. An effective PFE correction eliminates this kind of fake quenching and transforms the quenching plots recorded at different wavelengths of observation into one graph (PFE corrected). This graph still pretends larger quenching than actually results from the dynamic and static quenching process. The correction for PrFE, finally, excludes the remaining contributions of fake quenching and leads to one graph, upon which further determination of quenching constants is based.

The symmetry of mathematical expression (4) implies that a determination of the dynamic and static quenching constants by nonlinear regression works only if both quantities deviate considerably from each other in magnitude. The portion of dynamic quenching at T = 300 K was determined directly by measurements of fluorescence lifetimes. The values represented in Fig. 4 are characteristic of a diffusion-controlled process with K_{dyn} = 18.8 L mol^{-1}. Using this value we approximated the static quenching constant for the same temperature as K_{stat} = 4.0 L mol^{-1}. The monoexponential decay of fluorescence present with all quencher concentrations and the linearity of the Stern–Volmer plots of lifetimes exclude the occurrence of a transient quenching term.

On the basis of a diffusion-controlled process and the temperature dependence of solvent viscosity, the dynamic quenching constants for other temperatures were calculated.

These values together with the corresponding values of static quenching constants obtained from steady-state measurements are given in Table I. From the temperature dependence of the static quenching constant

(see Fig. 5), it follows, according to Eq. (5), that the Gibbs energy of association of the quenching complex amounts to $\Delta G_{stat} = -0.86$ kJ mol^{-1}. Comparing this value with the equilibrium constant of complex formation found by absorption spectroscopy shows that the static quenching constant is larger in magnitude (see also Ref. 9) but linked with a lower value of the Gibbs energy ($\Delta G_{CT} = -2.86$ kJ mol^{-1}).

Absorption spectroscopy reveals only the ionic state of the ground-state complex. This is the covalent state distinguished by larger distances between interacting molecules which becomes effective for fluorescence. A comparison of constants clarifies the contribution of the ionic bond structure to the mesomerism of the complex. The stronger interaction of the ionic bond structure accounts for the higher value of the Gibbs energy.

The equilibrium of CT complex formation is displaced by falling temperatures against the components (K_{stat}), and in addition, there is a simultaneous drive of the equilibrium of the superimposed ionic and covalent bindings inside the complex toward the ionic structure.

REFERENCES

1. R. Foster (1969) *Organic Charge-Transfer Complexes*, Academic Press, New York.
2. G. Junghähnel (1962) *Habilitationsschrift*, FSU, Jena.
3. D. Rehm and A. Weller (1969) *Ber. Bunsen-Ges. Phys. Chem.* **73**, 834.
4. J. R. Lakowicz (1983) *Principles of Fluorescence Spectroscopy*, Plenum Press, New York.
5. W. R. Ware (1962) *J. Phys. Chem.* **66**, 455–458.
6. P. Hentzschel and A. R. Watkins (1976) *J. Phys. Chem.* **80**, 494–500.
7. M. M. Puchalski, M. J. Morra, and R. von Wandruszka (1991) *Fresenius J. Anal. Chem.* **340**, 341–344.
8. C. A. Parker (1968) *Photoluminescence of Solutions*, Elsevier, New York.
9. P. G. Sennikov, V. A. Kuznezov, and A. N. Egorochkin (1981) *Adv. Mol. Interact. Proc.* **20**, 89.